

# Autonomous Navigation of AGVs in Automated Container Terminals

Yong-Shik Kim<sup>\*</sup> · Keum-Shik Hong<sup>\*\*</sup>

<sup>\*</sup>Dept. of Mechanical and Intelligent Systems Engineering, Pusan National University, Busan 609-735, Korea

<sup>\*\*</sup>School of Mechanical Engineering, Pusan National University, Busan 609-735, Korea

**ABSTRACT :** In this paper, an autonomous navigation system for autonomous guided vehicles (AGVs) operated in an automated container terminal is designed. The navigation system is based on the sensors detecting the range and bearing. The navigation algorithm used is an interacting multiple model (IMM) algorithm to detect other AGVs and avoid other obstacles using informations obtained from multiple sensors. As models to detect other AGVs (or obstacles), two kinematic models are derived: Constant velocity model for linear motion and constant speed turn model for curvilinear motion. For constant speed turn model, an unscented Kalman filter (UKF) is used because of drawbacks of the extended Kalman filter (EKF) in nonlinear system. The suggested algorithm reduces the root mean squares error for linear motions, while it can rapidly detect possible turning motions.

**KEY WORDS :** AGV, hybrid, IMM, nonlinear filtering, extended Kalman filter, unscented filter, navigation

## 1. Introduction

In container terminals, AGVs could be used to replace the manually driven trucks that transport containers within the terminal (Ioannou et al., 2001). A photograph of an AGV with load is shown in Fig. 1. While the automation of vehicles and trucks on highways does not have strong support of manufacturers due to liability issues and the complexity of the environment in which they have to operate, the use of automated trucks at low speeds in a restricted environment such as a terminal is a completely different story. The low speed characteristics of AGVs together with the restricted area they have to operate in makes the overall problem much simpler to solve. Therefore, the use of AGVs as container handling devices in terminals is feasible from the point of view of technology and has a strong potential to improve efficiency and reduce labor cost.

The ability to predict the motion of other AGVs (or obstacles) accurately in the terminal environment can improve the controller's ability to adapt smoothly to the behavior of those AGVs (or obstacles) preceding it (Madhavan and Durrant Whyte, 2004; Zhang et al., 2000).

This ability to predict motions is dependent on how well the sensors of an AGV can detect other AGVs (or obstacles). In order to detect other AGVs or avoid obstacles using the object information obtained from multiple sensors, tracking techniques based on Bayesian approach is usually used (Bar Shalom et al., 2001). Tracking a maneuvering target is a well established topic in the target tracking literature.

Techniques tracking a maneuvering target are used in many tracking and surveillance systems as well as in applications where reliability is a main concern (Bar Shalom et al., 2001; Li and Bar Shalom, 1993). A number of multiple model techniques to track a maneuvering target have been proposed in the literature using interactive multiple models (IMM) algorithm (Bar Shalom et al., 2001; Li and Bar Shalom, 1993).

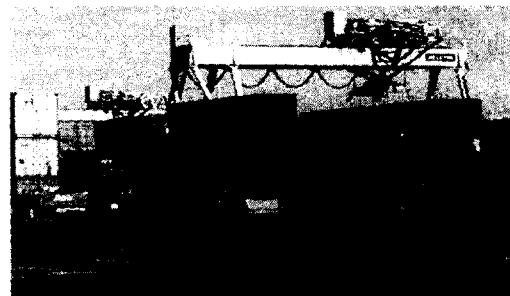


Fig. 1 Photograph of AGV in an automated container terminal.

Generally, target motion models can be divided into

\* imyjklaf@pusan.ac.kr (051)510-1481

\*\* kshong@pusan.ac.kr (051)510-2454

two subcategories: a uniform motion model and a maneuvering model. For tracking a maneuvering target, a validation method of a new type of flight mode was presented in (Nabaa and Bishop, 2000). Semerdjiev and Mihaylova (2000) have discussed variable and fixed structure augmented IMM algorithms, while a fixed structure was only discussed in (Li and Bar-Shalom, 1993), and applied them to a maneuvering ship tracking problem by augmenting the turn rate error.

In this paper, because of these drawbacks of the AIMM EKF, an unscented Kalman filter (UKF) (Julier et al, 2000; Ristic and Arulampalam, 2003) replacing the EKF is used for the curvilinear model. The algorithm itself uses the same AIMM logic, but the model-matched EKF is replaced by the model-matched UKF.

The objective of this paper is to design an UKF for curvilinear motions in an IMM algorithm to detect and avoid other AGVs for the autonomous navigation of an AGV in a automated port.

The main contributions of this paper are as follows: First, in an automated container terminal, the IMM algorithm as a navigation algorithm for AGVs to navigate autonomously is provided. Second, two kinematic models for possible navigation patterns of AGVs are derived: Constant velocity model for linear motion and constant speed turn model for curvilinear motion are discussed. Third, for constant speed turn model, an UKF is used because of the drawbacks of the EKF. Fourth, the suggested algorithm reduces the root mean squares error in the case of rectilinear motions and detects the occurrence of maneuvering quickly in the case of turning motions.

This paper is organized as follows: In Section 2, we provide various navigation patterns of AGV, a stochastic hybrid system is formulated, and two kinematic models are discussed. We then compare an UKF with an EKF for constant speed turn model in an IMM algorithm in Section 3. Section 4 concludes the paper.

## 2. Problem Formulation

### 2.1 Driving Patterns

Fig. 2 depicts various driving patterns of an AGV: straight line and curve, cut-in/out, and u-turn. All these

patterns can be represented by a combination of a constant velocity rectilinear motion, a constant acceleration rectilinear motion, a constant angular velocity curvilinear motion, and a constant angular acceleration curvilinear motion. As kinematic models for describing these motions, two stochastic models will be investigated: one for rectilinear motion and another for curvilinear motion. Typical navigation patterns are described briefly as follows:

i) Straight line and curve: In this situation, the AGV detects a preceding AGV that follows straight lines and curves on a curved road (Lauffenburger et al., 2003; Rajamani et al., 2003).

ii) Cut-in/out: The cut-in/out means the situation that a maneuvering AGV cuts in (or out) to (or from) the lane while the AGV is tracking other AGV. In this situation, detecting of up to three surrounding AGVs are assumed: one in front of it, one in the left, and one in the right. In this case, the target AGV changes its motion from a rectilinear motion to a curvilinear motion and then back to a rectilinear motion.

iii) U-turn: This situation occurs when the target AGV changes its driving direction by 180°. The u-turn consists of three routes as follows: The target AGV moves rectilinearly, undergoes a uniform circular turning up to 180° with a constant yaw rate, and then converts to a rectilinear motion in the opposite direction.

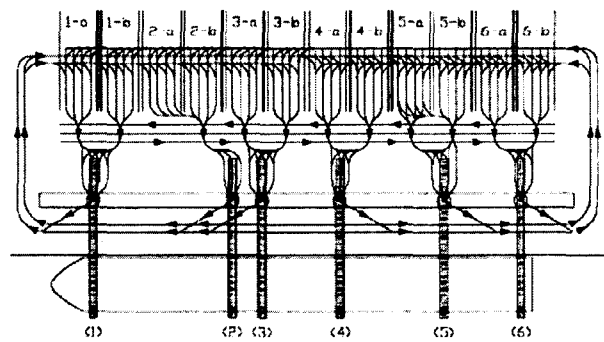


Fig. 2 Various driving patterns of an AGV (Duinkerken et al., 2002).

### 2.2 Stochastic Hybrid System

Following the work of (Li and Bar Shalom, 1993), a stochastic hybrid system with additive noise is considered as follows:

$$\mathbf{x}(k) = f[k-1, \mathbf{x}(k-1), \mathbf{m}(k)] + g[k-1, \mathbf{x}(k-1), \mathbf{v}[k-1, \mathbf{m}(k)], \mathbf{m}(k)] \quad (1)$$

with noisy measurements

$$z(k) = h[k, x(k), m(k)] + w[k, m(k)] \quad (2)$$

where  $x(k) \in \mathcal{R}^{n_x}$  is the state vector including the position, velocity, and yaw rate of the vehicle at discrete time  $k$ .  $m(k)$  is the scalar-valued modal state (driving mode index) at instant  $k$ , which is a homogeneous Markov chain with probabilities of transition given by

$$P\{m_j(k+1) | m_i(k)\} = \pi_{ij}, \quad \forall m_i, m_j \in \mathbf{M} \quad (3)$$

where  $P\{\cdot\}$  denotes probability and  $\mathbf{M}$  is the set of modal states, i.e., constant velocity, constant acceleration, constant angular rate turning with a constant radius of curvature, etc. The considered system is hybrid since the discrete events  $m(k)$  appears in the system. In the adaptive cruise control,  $m(k)$  denotes a driving mode of the preceding vehicle in effect during the sampling period ending at  $k$ , i.e., the time period  $[t_{k-1}, t_k]$ . The event that a mode  $m_j$  is in effect at time  $k$  is denoted as

$$m_j(k) \stackrel{\Delta}{=} \{m(k) = m_j\}. \quad (4)$$

$z(k) \in \mathcal{R}^{n_z}$  is the vector-valued noisy measurements from the sensor at time  $k$ , which is mode-dependent.  $v[k-1, m(k)] \in \mathcal{R}^{n_v}$  is the mode-dependent process noise sequence with mean  $\bar{v}[k-1, m(k)]$  and covariance  $Q[k-1, m(k)]$ .  $w[k, m(k)] \in \mathcal{R}^{n_z}$  is the mode-dependent measurement noise sequence with mean  $\bar{w}[k, m(k)]$  and covariance  $R[k, m(k)]$ . Finally  $f$ ,  $g$ , and  $h$  are nonlinear vector-valued functions.

### 2.3 Two Kinematic Models

The concept of using noise driven kinematic models comes from the fact that noises with different levels of variance can represent different motions. A model with high variance noise can capture maneuvering motions, while a model with low variance noise represents uniform motions. The multiple models approach assumes that a model can capture the complex system behavior better than others at an instant.

Two kinematic models for rectilinear and curvilinear motions are now derived: First, assuming that accelerations in the steady state are quite small (abrupt motions like a sudden stop or a collision are not covered), linear accelerations or decelerations can be reasonably well covered by process noises with the constant velocity model. That is, the constant velocity model plus a zero mean noise with an appropriate

covariance representing the magnitude of acceleration can handle uniform motions on the road. In discrete time, the constant velocity model with noise is given by

$$x(k) = \begin{bmatrix} 1 & T & 0 & 0 \\ 0 & 1 & 0 & 0 \\ 0 & 0 & 1 & T \\ 0 & 0 & 0 & 1 \end{bmatrix} x(k-1) + \begin{bmatrix} \frac{1}{2}T^2 & 0 \\ T & 0 \\ 0 & \frac{1}{2}T^2 \\ 0 & T \end{bmatrix} v(k-1) \quad (5)$$

where  $T$  is the sampling time (0.01 sec),  $x(k)$  is the state vector including the position and velocity of the preceding vehicle in the longitudinal ( $\xi$ ) and lateral ( $\eta$ ) directions at discrete time  $k$ , i.e.,

$$x(k) = [\xi(k) \quad \dot{\xi}(k) \quad \eta(k) \quad \dot{\eta}(k)]^T \quad (6)$$

with  $\xi$  and  $\eta$  denoting the orthogonal coordinates of the horizontal plane; and  $v$  is a zero-mean Gaussian white noise representing the accelerations with an appropriate covariance  $Q$ . If  $v(k)$  is the acceleration increment during the  $k$ th sampling period, the velocity during this period is calculated by  $v(k)T$ , and the position is altered by  $v(k)T^2/2$ .

Secondly, a discrete-time model for turning is derived from a continuous time model for the coordinated turn motion (Bar Shalom et al., 2001, p. 183). A constant speed turn is a turn with a constant yaw rate along the road of constant radius of curvature. However, the curvatures of actual roads are not constant. Hence, a fairly small noise is added to a constant speed turn model for the purpose of capturing the variation of the road curvature. The noise in the model represents the modeling error such as the presence of angular acceleration and not constant radius of curvature. For a vehicle turning with a constant angular rate and moving with constant speed (the magnitude of the velocity vector is constant), the kinematic equations in the  $(\xi, \eta)$  plane are

$$\ddot{\xi}(t) = -\omega\dot{\eta}(t), \quad \ddot{\eta}(t) = \omega\dot{\xi}(t) \quad (7)$$

where  $\ddot{\xi}(t)$  is the normal (longitudinal) acceleration and  $\ddot{\eta}(t)$  denotes the tangential acceleration, and  $\omega$  is the constant yaw rate ( $\omega > 0$  implies a counterclockwise turn). The tangential component of the acceleration is equal to the rate of change of the speed, i.e.,  $\dot{\eta}(t) = d\eta(t)/dt = d(\omega\xi(t))/dt$ , and the normal component is defined as the square of the speed in the tangential direction divided by the radius of curvature of the path, i.e.,  $\ddot{\xi}(t) = -\dot{\eta}^2(t)/\xi(t) = -\omega^2\xi^2(t)/\xi(t)$  where  $\dot{\eta}(t) = \omega\xi(t)$ .

The state space representation of (7) with the state vector defined by  $\mathbf{x}(k) = [\xi(k) \ \dot{\xi}(k) \ \eta(k) \ \dot{\eta}(k)]^T$  becomes

$$\dot{\mathbf{x}}(t) = \mathbf{A}\mathbf{x}(t) \quad (8)$$

where

$$\mathbf{A} = \begin{bmatrix} 0 & 1 & 0 & 0 \\ 0 & 0 & 0 & -\omega \\ 0 & 0 & 0 & 1 \\ 0 & \omega & 0 & 0 \end{bmatrix}$$

The state transient matrix of the system (8) is given by

$$e^{\mathbf{A}t} = \begin{bmatrix} 1 & \frac{\sin \omega t}{\omega} & 0 & \frac{1 - \cos \omega t}{\omega} \\ 0 & \cos \omega t & 0 & -\frac{\sin \omega t}{\omega} \\ 0 & \frac{1 - \cos \omega t}{\omega} & 1 & \frac{\sin \omega t}{\omega} \\ 0 & \frac{\sin \omega t}{\omega} & 0 & \cos \omega t \end{bmatrix} \quad (9)$$

It is remarked that if the angular rate  $\omega$  in (7) is time varying, (9) wouldn't be true any more. In the sequel, following the approach in (Bar-Shalom et al., 2001, p. 466), a "nearly" constant speed turn model in discrete-time domain is introduced. In this approach, the model itself is motivated from (9) but the angular rate is allowed to vary.

A new state vector by augmenting the angular rate  $\omega(k)$  to the state vector of (7) is defined as follows:

$$\mathbf{x}^a(k) = [\xi(k) \ \dot{\xi}(k) \ \eta(k) \ \dot{\eta}(k) \ \omega(k)]^T. \quad (10)$$

Then, the nearly constant speed turn model is defined as follows [1, p. 467]:

$$\mathbf{x}^a(k) = \begin{bmatrix} 1 & \frac{\sin \omega(k-1)T}{\omega(k-1)} & 0 & \frac{1 - \cos \omega(k-1)T}{\omega(k-1)} & 0 \\ 0 & \cos \omega(k-1)T & 0 & -\frac{\sin \omega(k-1)T}{\omega(k-1)} & 0 \\ 0 & \frac{1 - \cos \omega(k-1)T}{\omega(k-1)} & 1 & \frac{\sin \omega(k-1)T}{\omega(k-1)} & 0 \\ 0 & \frac{\sin \omega(k-1)T}{\omega(k-1)} & 0 & \cos \omega(k-1)T & 0 \\ 0 & 0 & 0 & 0 & 1 \end{bmatrix} \mathbf{x}^a(k-1) + \begin{bmatrix} \frac{T^2}{2} & 0 & 0 \\ \frac{T}{1} & 0 & 0 \\ 0 & \frac{T^2}{2} & 0 \\ 0 & T & 0 \\ 0 & 0 & T \end{bmatrix} \nu^a(k-1) \quad (11)$$

where superscript  $a$  denotes the augmented value.

### 3. Proposed Unscented Kalman Filter for Turning Motion

#### 3.1 The EKF for Constant Speed Turn Model

Since the model in (11) is nonlinear, the estimation

of the state (10) will be done via the EKF. The nearly constant speed turn model of (11) can be rewritten as follows:

$$\mathbf{x}^a(k) = f^a[\mathbf{x}^a(k-1), \omega(k-1)] + \mathbf{G}(k-1)\nu^a(k-1), \quad (12)$$

where the function  $f^a(\cdot)$  is known and remains unchanged during the estimation procedure. The noise transition matrix  $\mathbf{G}(k-1)$  is the same form as the one given in (11). To obtain the predicted state  $\hat{\mathbf{x}}^a(k|k-1)$ , the nonlinear function in (12) is expanded in Taylor series around the latest estimate  $\hat{\mathbf{x}}^a(k-1|k-1)$  with terms up to first order to yield the first order EKF. The vector Taylor series expansion of (12) up to first order is

$$\mathbf{x}^a(k) = f^a[\hat{\mathbf{x}}^a(k-1|k-1), \omega(k-1)] + f_{x^a}^a(k-1)[\mathbf{x}^a(k-1) - \hat{\mathbf{x}}^a(k-1|k-1)] + \text{HOT} + \mathbf{G}(k-1)\nu^a(k-1) \quad (13)$$

where HOT represents the higher-order terms and

$$f_{x^a}^a(k-1) = [\nabla_{x^a} f^a(x^a, \omega)]^T |_{x^a = \hat{x}^a(k-1|k-1)}$$

$$= \begin{bmatrix} 1 & \frac{\sin \hat{\omega}(k-1)T}{\hat{\omega}(k-1)} & 0 & \frac{1 - \cos \hat{\omega}(k-1)T}{\hat{\omega}(k-1)} & f_{\omega,1}(k-1) \\ 0 & \cos \hat{\omega}(k-1)T & 0 & -\frac{\sin \hat{\omega}(k-1)T}{\hat{\omega}(k-1)} & f_{\omega,2}(k-1) \\ 0 & \frac{1 - \cos \hat{\omega}(k-1)T}{\hat{\omega}(k-1)} & 1 & \frac{\sin \hat{\omega}(k-1)T}{\hat{\omega}(k-1)} & f_{\omega,3}(k-1) \\ 0 & \frac{\sin \hat{\omega}(k-1)T}{\hat{\omega}(k-1)} & 0 & \cos \hat{\omega}(k-1)T & f_{\omega,4}(k-1) \\ 0 & 0 & 0 & 0 & 1 \end{bmatrix} \quad (14)$$

is the Jacobian of the vector  $f$  evaluated at the latest estimate of the state. The partial derivatives with respect to  $\omega$  are given by

$$f_{\omega,1} = \frac{T \hat{\xi}(k-1|k-1) \cos \hat{\omega}(k-1)T}{\hat{\omega}(k-1)} \frac{\hat{\xi}(k-1|k-1) \sin \hat{\omega}(k-1)T}{\hat{\omega}(k-1)^2} - \frac{T \hat{\eta}(k-1|k-1) \sin \hat{\omega}(k-1)T}{\hat{\omega}(k-1)} \frac{\hat{\eta}(k-1|k-1)(-1 + \cos \hat{\omega}(k-1)T)}{\hat{\omega}(k-1)^2},$$

$$f_{\omega,2} = -T \hat{\xi}(k-1|k-1) \sin \hat{\omega}(k-1)T - T \hat{\eta}(k-1|k-1) \cos \hat{\omega}(k-1)T,$$

$$f_{\omega,3} = \frac{T \hat{\xi}(k-1|k-1) \sin \hat{\omega}(k-1)T}{\hat{\omega}(k-1)} \frac{\hat{\xi}(k-1|k-1)(1 - \cos \hat{\omega}(k-1)T)}{\hat{\omega}(k-1)^2} + \frac{T \hat{\eta}(k-1|k-1) \cos \hat{\omega}(k-1)T}{\hat{\omega}(k-1)} \frac{\hat{\eta}(k-1|k-1) \sin \hat{\omega}(k-1)T}{\hat{\omega}(k-1)^2},$$

$$f_{\omega,4} = T \hat{\xi}(k-1|k-1) \cos \hat{\omega}(k-1)T - T \hat{\eta}(k-1|k-1) \sin \hat{\omega}(k-1)T. \quad (15)$$

Based on the above expansion, the state prediction and state prediction covariance in the EKF are

$$\hat{\mathbf{x}}^a(k|k-1) = f^a[\hat{\mathbf{x}}^a(k-1|k-1), \omega(k-1)], \quad (16)$$

$$\mathbf{P}^a(k|k-1) = f_{x^a}^a(k-1) \mathbf{P}^a(k-1|k-1) f_{x^a}^a(k-1) + \mathbf{G}(k-1) \mathbf{Q}^a(k-1) \mathbf{G}'(k-1) \quad (17)$$

where  $Q^a$  is the covariance of the process noise in (12). The details of the EKF in an IMM algorithm during one cycle are given in Table 1.

Table 1. Summary of the EKF in an IMM algorithm (one cycle).

Filtering	
predicted estimate	$\hat{x}^a(k k-1) = f^a(\hat{x}_0^a(k-1 k-1), \omega(k-1))$
predicted covariance	$P^a(k k-1) = f_{x^a}^a(k-1)P_0^a(k-1 k-1)f_{x^a}^{a'}(k-1) + G(k-1)Q^a(k-1)G'(k-1)$
measurement residual	$\nu(k) = z(k) - H\hat{x}^a(k k-1)$
residual covariance	$S(k) = HP^a(k k-1)H' + R(k)$
filter gain	$K^a(k) = P^a(k k-1)H'S^{-1}(k)$
updated estimate	$\hat{x}^a(k k) = \hat{x}^a(k k-1) + K^a(k)\nu(k)$
updated covariance	$P^a(k k) = P^a(k k-1) - K^a(k)S(k)K^a(k)'$
likelihood function	$\Lambda = N[\nu; 0, S] =  2\pi S ^{-1/2} e^{-\frac{1}{2}\nu'S^{-1}\nu}$
mode probability	$\mu = \frac{\mu^- \Lambda}{\sum_i \mu_i^- \Lambda_i}$

### 3.2 The UKF for Constant Speed Turn Model

Because of the well-known drawbacks of the EKF, the unscented Kalman filter for constant speed turn models is used (Julier et al, 2000; Ristic and Arulampalam, 2003).

Similar to the EKF, the UKF is a recursive minimum mean square error estimator. But unlike the EKF, which only uses the first-order terms in the Taylor series expansion of the non-linear measurement equation, the UKF uses the true measurement model and approximates the distribution of the state vector. This state distribution is still represented by a Gaussian density, but it is specified with a set of deterministically chosen sample (or sigma) points. The sample points completely capture the true mean and covariance of the Gaussian random vector. When propagated through any non-linear system, the sample points capture the posterior mean and covariance accurately to the second order. The main building block of the UKF is the unscented transform, described below.

The unscented transform is a method for calculating the statistics of a random vector which undergoes a non-linear transformation. Let  $x \in \mathcal{R}^{n_x}$  be a random vector,  $p: \mathcal{R}^{n_x} \rightarrow \mathcal{R}^{n_y}$  a non-linear transformation and  $y = p(x)$ . Assume the mean and the covariance of  $x$  are

$\bar{x}$  and  $P_x$ , respectively. The procedure for calculating the first two moments of  $y$  using the unscented transform is as follows (Julier et al, 2000):

1) Compute  $(2n_x + 1)$  sigma points  $\chi_i$  and their weights  $W_i$ :

$$\begin{aligned} \chi_0 &= \bar{x}, & W_0 &= \frac{\kappa}{n_x + \kappa}, & i &= 0, \\ \chi_i &= \bar{x} + (\sqrt{(n_x + \kappa)P_x})_i, & W_i &= \frac{1}{2(n_x + \kappa)}, & i &= 1, \dots, n_x, \\ \chi_i &= \bar{x} - (\sqrt{(n_x + \kappa)P_x})_i, & W_i &= \frac{1}{2(n_x + \kappa)}, & i &= n_x + 1, \dots, 2n_x. \end{aligned} \quad (18)$$

where  $\kappa$  is a scaling parameter for fine tuning the higher order moments of the approximation and  $(\sqrt{(n_x + \kappa)P_x})_i$  is the  $i$ th row or column of the matrix square root of  $(n_x + \kappa)P_x$ .

2) Propagate each sigma point through the non-linear function

$$\zeta_i = p(\chi_i) \quad (i = 0, \dots, 2n_x). \quad (19)$$

3) Calculate the mean and covariance of  $y$  as follows:

$$\begin{aligned} \bar{y} &= \sum_{i=0}^{2n_x} W_i \zeta_i, \\ P_y &= \sum_{i=0}^{2n_x} W_i (\zeta_i - \bar{y})(\zeta_i - \bar{y})'. \end{aligned} \quad (20)$$

Next the UKF filter for constant speed turn model is derived as follows:

1) Using (18), compute sigma points  $\chi_i(k-1|k-1)$  and weights  $W_i$  ( $i = 0, \dots, 2n_x$ ) corresponding to  $\hat{x}^a(k-1|k-1)$  and  $P^a(k-1|k-1)$ .

2) Predict sigma points using state equation (12) as follows:

$$\chi_i(k|k-1) = f^a[\chi_i(k-1|k-1), \omega(k-1)]. \quad (21)$$

3) Compute the predicted mean and covariance of the state variable  $\hat{x}^a(k|k-1)$  and  $P^a(k|k-1)$ , using prediction sigma points  $\chi_i(k|k-1) \in \mathcal{R}^{n_x}$  and their weights  $W_i$   $i = 0, \dots, 2n_x$ .

$$\begin{aligned} \hat{x}^a(k|k-1) &= \sum_{i=0}^{2n_x} W_i \chi_i(k|k-1), \\ P^a(k|k-1) &= Q^a + \sum_{i=0}^{2n_x} W_i [\chi_i(k|k-1) - \hat{x}^a(k|k-1)] \\ &\quad \cdot [\chi_i(k|k-1) - \hat{x}^a(k|k-1)]'. \end{aligned} \quad (22)$$

4) Predict measurement sigma points  $\mathfrak{Z}_i(k|k-1)$  using (2) as follows:

$$\mathfrak{Z}_i(k|k-1) = h[\chi_i(k|k-1), \omega(k)]. \quad (23)$$

5) Predict measurement and covariances

$$\hat{z}^a(k|k-1) = \sum_{i=0}^{2n} \mathcal{W}_i \mathcal{Z}_i(k|k-1),$$

$$P_{zz}^a = R(k) + \sum_{i=0}^{2n} \mathcal{W}_i [\mathcal{Z}_i(k|k-1) - \hat{z}^a(k|k-1)] [\mathcal{Z}_i(k|k-1) - \hat{z}^a(k|k-1)]',$$

$$P_{xz}^a = \sum_{i=0}^{2n} \mathcal{W}_i [\chi_i(k|k-1) - \hat{x}^a(k|k-1)] [\mathcal{Z}_i(k|k-1) - \hat{z}^a(k|k-1)]' \quad (24)$$

where  $P_{zz}^a$  and  $P_{xz}^a$  are, respectively, the covariance matrix of the measurement and the cross-covariance of the measurement and state variable.

6) Compute the filter gain as

$$K^a(k) = P_{xz}^a (P_{zz}^a)^{-1}. \quad (25)$$

Update the UKF filter with measurement  $z(k)$  as

$$\hat{x}^a(k|k) = \hat{x}^a(k|k-1) + K^a(k) [z(k) - \hat{z}^a(k|k-1)], \quad (26)$$

$$P^a(k|k) = P^a(k|k-1) - K^a(k) P_{zz}^a K'^a(k). \quad (27)$$

Note that the UKF requires computation of a matrix square root in (18), which can be done using Cholesky factorization.

## 4. Conclusions

In this paper, a tracking algorithm for AGVs operated in the automated container terminal was designed. As models to detect other AGVs, two kinematic models were derived: Constant velocity model for linear motion and constant speed turn model for curvilinear motion. For constant speed turn model, an unscented Kalman filter was used because of the drawbacks of the extended Kalman filter in nonlinear systems. The suggested algorithm reduced the root mean squares error for linear motions, while it can rapidly detect possible turning motions.

## Acknowledgements

This work was supported by the Ministry of Science and Technology of Korea under a program of the National Research Laboratory, grant number NRL M1-0302-00-0039-03-J00-00-023-10.

## References

[1] Bar-Shalom, Y., Li, X., and Kirubarajan, T. (2001).

*Estimation with Applications to Tracking and Navigation*, John Wiley & Sons, INC, New York, Chapter 11, pp. 421-490.

[2] Ioannou, P. A., Jula, H., and Dougherty, E. Jr. (2001), "Advanced material handling: Automated guided vehicles in agile ports," Technical Report, Center for Advanced Transportation Technologies, University of Southern California.

[3] Julier, S. J., Uhlmann, J. K., and Durrant Whyte, H. F. (2000), "A new method for the nonlinear transformation of means and covariances in filters and estimators," *IEEE Trans. on Automatic Control*, Vol. 45, No. 3, pp. 477-482.

[4] Lauffenburger, J. Ph., Basset, M., Coffin, F., and Gissingner, G. L. (2003), "Driver-aid system using path-planning for lateral vehicle control," *Control Engineering Practice*, Vol. 11, No. 2, pp. 217-231.

[5] Li, X. and Bar Shalom, Y. (1993), "Design of an interacting multiple model algorithm for air traffic control tracking," *IEEE Trans. on Control Systems Technology*, Vol. 1, No. 3, Sept. 1993, pp. 186-194.

[6] Madhavan, R. and Durrant-Whyte, H. F. (2004), "Natural landmark based autonomous vehicle navigation," *Robotics and Autonomous Systems*, Vol. 46, pp. 79-95.

[7] Nabaa, N. and Bishop, R. H. (2000), "Validation and comparison of coordinated turn aircraft maneuver models," *IEEE Transactions on Aerospace and Electronic Systems*, Vol. 36, No. 1, pp. 250-259.

[8] Rajamani, R., Zhu, C., and Alexander, L. (2003), "Lateral control of a backward driven front steering vehicle," *Control Engineering Practice*, Vol. 11, No. 5, pp. 531-540.

[9] Semerdjiev, E. and Mihaylova, L. (2000), "Variable- and fixed-structure augmented interacting multiple-model algorithms for manoeuvring ship tracking based on new ship models," *International Journal of Applied Mathematics and Computer Science*, Vol. 10, No. 3, pp. 591-604.

[10] Zhang, W. W., Zhuang, B. H., and Zhang, Y. (2000), "Novel navigation sensor for autonomous guide," *Optical Engineering*, Vol. 39, No. 9, pp. 2511-2516.

[11] Duinkerken, M. B., Evers, J. J. M., and Ottjes, J. A. (2002), "Improving quay transport on automated container terminals," *IASTED*.